

Energy Optimal Trajectory Planning of Biped Walking Motion

Rongqiang Liu¹ and Kyosuke Ono²

^{1,2}Dept. of Mechanical Science and Engineering, Tokyo Institute of Technology
2-12-1 Ohokayama Meguro-ku Tokyo, 152-8552 Japan

¹E-mail: liurq@stu.mech.titech.ac.jp, ²E-mail: ono@mech.titech.ac.jp

Abstract

This paper describes an optimal trajectory planning of walking locomotion for a biped mechanism system which has thighs, shanks and small feet. We model the mechanism to be a 3-DOF link system composed of an inverted pendulum and a 2-DOF swing leg. The locomotion of the swing and supported legs is solved by the optimal trajectory planning method based on the function approximation method. It was found that the lowest energy walking motion can be obtained at the one step period of 0.586s similar to the human walking when the ankle is a passive joint.

1 Introduction

Many studies have been published on dynamic biped locomotion mechanism, in which there are many successful examples to realize dynamic walking of biped robots. Mita et al. built a seven-link biped walker and realized dynamic biped walking by using linear optimal state regulator theory^[1]. As a result, one step took one second when the step length was shorter than 20cm. Furusho et al. proposed a hierarchical control strategy for their biped robot and realized high speed movement^[2]. The local feedback which makes the total system robust was implemented at the low level. The stability of steady walking was examined by using the reduced order model. Shih studied dynamics of a 7-DOF biped walking robot which included variable length legs and a translational balance weight in the body^[3]. He presented a piecewise cubic polynomials method to generate a trajectory by constraining the location of the ZMP and showed an experimental result of dynamic walking with a speed of 16cm/s.

However, most of the previous control algorithms are very complicated, and the walking stability and speed are not as good as expected. On the other hand, human biped walking has been con-

sidered to be robust and efficient. The human walking pattern can be described similarly by the simplest inverted pendulum model in gravitational field^[4]. Therefore, human utilizes its gravity skillfully to achieve efficient walking. Miura and Shimoyama developed biped robots named BIPER-3 and BIPER-4, and proposed a control method based on the inverted pendulum principle to realize dynamic walking^[5]. McGeer demonstrated a passive biped walking mechanism which walked down along a ramp and utilized its gravitational potential energy as input power of walking^[6]. It is indicated that the biped walking under gravitational field has a natural gait and the walking is generated as a limit cycle of non-linear system. Based on natural dynamics concept of a biped system, Pratt et al. studied a planar biped walking control by the virtual model method. They exploited the natural dynamics of human legs to simplify the control algorithm greatly^[7].

Ono and Okada proposed self-excitation of natural mode of vibration system and demonstrated an insect wing driven by the Van Der Pole self-excitation^{[8][9]}. They also proposed a biped mechanism which walked on a level ground with two single-link legs. The biped walking motion was realized by the swing roll motion of the upper body driven by a self-excited vibration system with asymmetric stiffness matrix^[10]. Moreover, Ono et al. described a self-excited biped mechanism with one actuator only at the hip and realized the natural dynamic walking motion with a speed of about 3km/h on a level ground^[11].

Since a natural walking locomotion means such an efficient motion that the energy consumption is the lowest, it is thought that the natural walking locomotion can be obtained as a motion of a biped mechanism that consumes the lowest possible energy. Thus, our main concern in this study is whether we can get a stable, efficient and natural walking motion and the lowest input torque at all joints, by means of an optimal trajectory planning method based on energy consumption mini-

1 Visiting Researcher, Associate Professor.
Harbin Institute of Technology, Harbin, China.

mization. Another concern is whether we can also obtain ideal walking motion even if we assume the ankle or knee joint to be a passive joint. In addition, we are interested in the similarity between the optimal walking motion solutions and actual human walking motion.

The trajectory planning problem can be solved by the variational method, the maximum principle or the dynamic programming method, but the state equations are very complicated and the convergence is difficult. Thus, we approximate the joint motion trajectory by a set of Hermite polynomials functions^[12], and convert the optimal trajectory planning problem into the boundary parameter optimization problem.

2 Analytical Method

In this section, we model a planar biped walking mechanism with thighs, shanks and small feet as shown in Figure 1 to be a 3-DOF link system. We disregard upper body above waist, because it has little effect on walking motion. Thus, the two legs are assumed to be directly connected each other through an actuator. We assume that both knee and ankle joints can be driven by individual actuators.

2.1 Model of a Biped Mechanism and Walking Motion

For the biped mechanism as shown in Figure 1, we assume that the knee joint of the supported leg is passively locked by means of a stopper mechanism to prevent the mechanism from collapse. The ankle of the supported leg is modeled as a rotating joint fixed on the ground, while the foot of the swing leg is neglected. The mechanism is modeled as a 3-DOF link system as shown in Figure 2, which consists of an inverted pendulum and a 2-DOF swing leg.

The one step walking locomotion is divided into three sections which have different phases of the walking mechanism as shown in Figure 3. In the first section from the posture 1 to 2, the swing leg swings from left to right as a 2-DOF pendulum until the swing leg becomes straight, avoiding collision with the ground, while the supported leg moves from left to right as a 1-DOF inverted pendulum. In the second section, it is assumed that the straight two legs move freely during the period t_2 from posture 2 to 3 until the swing leg touches the ground. In the third section, only the foot exchange is performed from posture 3 to 4 at the instant of collision of the swing leg. An efficient and natural walking motion of a 3-DOF walking

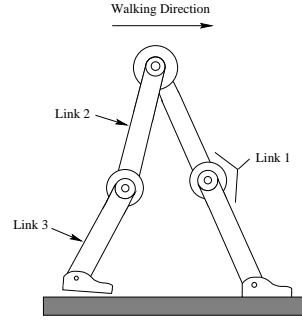


Figure 1: Biped walking mechanism

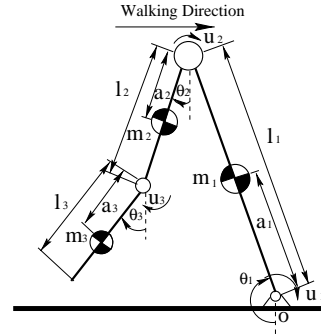


Figure 2: The model of biped walking mechanism

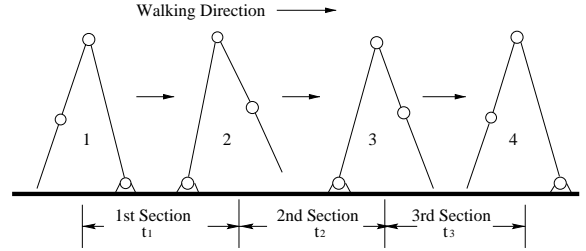


Figure 3: Sections of one step walking

mechanism in the first section is solved by the optimal trajectory planning method.

2.2 Basic Equations and Cyclic Walking Locomotion Condition

The equation of motion of the 3-DOF link system as shown in Figure 2 is written as follows:

$$[M]\{\ddot{\theta}\} + [c]\{\dot{\theta}^2\} + \{k\} = \{u\} \quad (1)$$

where $[M]$, $[c]$ and $\{k\}$ are calculated by the parameter values of the mechanism and the angular positions of the links, and $\{u\}$ is the input torque vector.

We assume that the foot exchange takes place instantly for the sake of analytical simplicity and the collision between the swing leg and the ground is perfect non-elastic collision. By using the impulse-momentum equations for translation and rotation,

the relationship of the link angular speeds between right before and after collision is obtained as follows.

$$[\mathbf{H}]\{\dot{\boldsymbol{\theta}}^-\} = [\mathbf{M}]\{\dot{\boldsymbol{\theta}}^+\} \quad (2)$$

where $[\mathbf{H}]$ is calculated by the parameter values of the mechanism and the angular positions of the links. In order to realize the cyclic walking locomotion, the angular speed $\dot{\boldsymbol{\theta}}^+$ right after the foot exchange must be the same as that at the beginning of the first section which is given as the initial condition. So the angular speed $\dot{\boldsymbol{\theta}}^-$ right before the foot exchange is solved by Eq. (2).

From Eq. (1), the equation of motion of 2-DOF link system in the second section is written in following.

$$\ddot{\boldsymbol{\theta}} = \mathbf{f}(\boldsymbol{\theta}, \dot{\boldsymbol{\theta}}) \quad (3)$$

To determine the end boundary condition of the first section, we adopt a backward time integration method. By integrating Eq. (3) from posture 3 to 2 during the second section and using Eq. (2), we have the relationship between the beginning and end boundary conditions.

2.3 Optimal Trajectory Planning Based on Function Approximation

In the first section, the walking motion of 3-DOF link system is solved by the optimal trajectory planning method^[12]. To minimize the energy consumption in the first section, we define the performance index function as follows.

$$J = \sum_{i=1}^3 k_{p_i} \int_0^{t_1} u_i^2(t) dt \quad (4)$$

where k_{p_i} is the weighting factor corresponding to joint i , and u_i is the input torque at joint i . Arranging Eq. (1), u_i is expressed as:

$$u_i = \Gamma_i(\boldsymbol{\theta}, \dot{\boldsymbol{\theta}}, \ddot{\boldsymbol{\theta}}) \quad (i = 1, 2, 3) \quad (5)$$

In order to compare the full-actuated and under-actuated systems, we solve this trajectory planning problem under three input conditions as follows.

1. No input at the ankle joint: $k_{p_1} = 0$ in (7); the constraint condition $u_1 = 0$.
2. No input at the knee joint: $k_{p_3} = 0$ in (7); the constraint condition $u_3 = 0$.
3. Input at all the joints: no constraint condition.

If the first section is divided into m subsections, then the joint motion trajectory in the j -th subsection is expressed as

Table 1: Link parameters

	1st link	2nd link	3rd link
Mass m_i [kg]	5.0	3.5	1.5
Link length l_i [m]	0.8	0.4	0.4
Inertia moment I_i [kgm ²]	0.35	0.054	0.02
Offset of mass center a_i [m]	0.56	0.09	0.20

$$\boldsymbol{\theta}_j(\mathbf{p}, t) = \mathbf{h}(t)^T \mathbf{p}_j \quad (j=1, \dots, m) \quad (6)$$

where $\mathbf{h}(t)$ is the Hermite base function vector of n_h order. In this paper, we take $n_h = 7$ and $m = 2$. \mathbf{p}_j is the boundary state variable vector. Therefore,

$$\mathbf{p}_j = \{\boldsymbol{\theta}_{j-1}^T, \boldsymbol{\theta}_j^T, \dot{\boldsymbol{\theta}}_{j-1}^T, \dot{\boldsymbol{\theta}}_j^T, \ddot{\boldsymbol{\theta}}_{j-1}^T, \ddot{\boldsymbol{\theta}}_j^T, \boldsymbol{\theta}_{j-1}^{(3)T}, \boldsymbol{\theta}_j^{(3)T}\}^T \quad (7)$$

where the number in the () is the derivative order number, $\boldsymbol{\theta}_{j-1}$, $\dot{\boldsymbol{\theta}}_{j-1}$ etc are the beginning boundary state variables of the j -th subsection, while $\boldsymbol{\theta}_j$, $\dot{\boldsymbol{\theta}}_j$ etc are the end boundary state variables of the j -th subsection. To satisfy the dynamic constraint condition of the passive joint, the input torque $u_k(t, \mathbf{p})$ of this joint must satisfy the condition that the projection of the $u_k(t, \mathbf{p})$ in the Hermite base functional space is zero. That is,

$$\mathbf{c}(\mathbf{p}) = \int_0^{t_1} u_k(t, \mathbf{p}) h_i(t) dt = 0 \quad (i = 1, \dots, n_h). \quad (8)$$

The constrained optimization problem as shown in (4) and (8) is solved iteratively until the ratio of difference of the successive value of \mathbf{p} becomes small enough.

3 Results and Discussions

We solve the optimal walking locomotion trajectory for the 3-DOF link system as shown in Figure 2 for various values of the second period t_2 under three input conditions, using the calculation method stated above. The parameter values of the mechanism are shown in Table 1, which are close to an adult human's data. In the iteration calculation, the convergence accuracy ε is chosen to be 1.0×10^{-10} .

First, we show the optimal solutions of walking motion under the constraint condition $u_1 = 0$. Figures 4, 5 and 6 show the stick figures and joint torque in the cases of $t_2=0.10s$, $0.12s$ and $0.13s$, respectively. Note that, the track of the swing leg is like a straight line which parallels the ground when $t_2 = 0.1s$, as shown in Figure 4(a). When the

t_2 is less than 0.09s, the teo track comes to collide with the ground, so the result could not be obtained. From the comparison of Figures 4, 5 and 6, it is clear that the larger the t_2 is, the higher the peak of the teo track. The calculation at $t_2 > 0.13s$ is unnecessary, because the higher the peak of the teo track, the larger the energy consumption value is. The joint input torque in Figure 4(b) is obviously smaller than that in Figures 5(b) and 6(b). In Figures 4(b), 5(b) and 6(b), we note that the u_1 is not zero. However, since the u_1 is orthogonal with the Hermite polynomial base functional space, the u_1 has no influence on the $\theta(\mathbf{p}, t)$. Because the u_1 satisfies Eq. (11). We confirmed that the same walking motion as in Figures 4(a), 5(a) and 6(a) can be obtained from forward dynamic simulation by using $u_1=0$ and the same u_2 and u_3 as in Figures 4(b), 5(b) and 6(b), respectively.

Next, we calculate optimal trajectory under the constraint condition $u_3 = 0$. Figure 7 shows the stick figure and input torque in the case of $t_2 = 0.10s$. During the iteration, the final constraint condition error is 1.0×10^{-4} , which is much worse than the required convergence accuracy of 1.0×10^{-10} . Sharp peak on the u_3 curve near the end of the first section is observed in Figure 7(b). Therefore, under no input torque at joint 3, the optimum joint motion trajectory which satisfies the required boundary condition could not be found. This indicates that some input torque at the knee is very important to generate an efficient walking motion.

Finally, we calculate the optimal trajectories when the torque is input at all three joint. The stick figures for $t_2 = 0.10$ and 0.13s are shown in Figure 8. The stick figures are very smooth in both two cases and are very similar to each other as shown in Figure 8. It is understood that the trajectory pattern and energy consumption are insensitive to the boundary condition in the full-actuated control system.

The value of the performance index in the 12 cases is shown in Figure 9. The energy consumption value in the full-actuated control system increases slowly with the increase in t_2 . When joint 1 is a passive joint, the energy consumption value increases quickly with an increase in t_2 . However the energy consumption shows the lowest value in all 12 cases when $u_1 = 0$ and $t_2 = 0.10s$, as seen in Figure 9. Therefore, this motion trajectory is considered to be the most optimal walking motion. It is interesting to note that a cyclic walking motion with the lowest energy consumption can be realized in an under-actuated control system as a kind of natural motion of a multi-link system, if a suitable boundary condition is adopted.

Of all the 12 examples, the period t_1 of the first

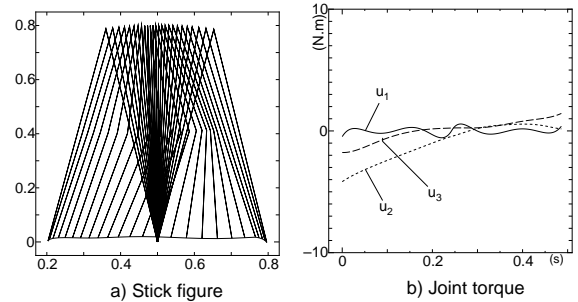


Figure 4: Computation results on $u_1 = 0$ and $t_2 = 0.10s$

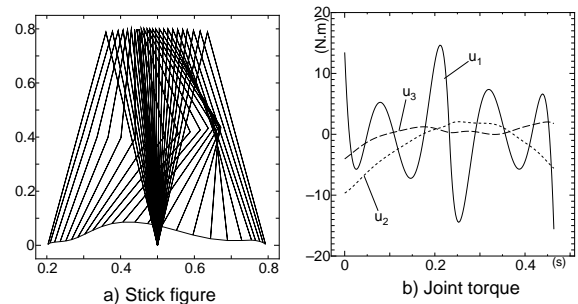


Figure 5: Computation results on $u_1 = 0$ and $t_2 = 0.12s$

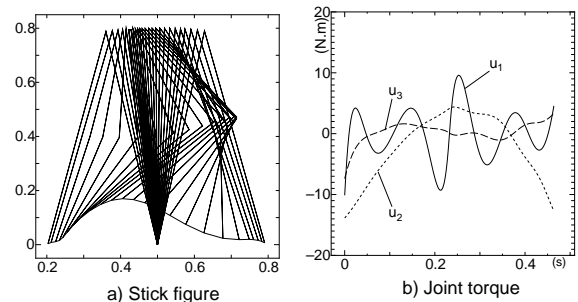


Figure 6: Computation results on $u_1 = 0$ and $t_2 = 0.13s$

section is within $0.462s \sim 0.486s$, while the one step walking period ($t_1 + t_2$) is within $0.582s \sim 0.596s$. This value is very close to the human walking period. Accordingly, it can be said that the optimal solution solved by the trajectory planning method described above is close to human walking locomotion.

4 Conclusions

In this paper, we computed the optimal joint motion trajectory for the 3-DOF biped walking mechanism, using the optimal trajectory planning method. From comparison of the computation results, the main conclusions are summarized as follows.

- (1) The computation results prove that the op-

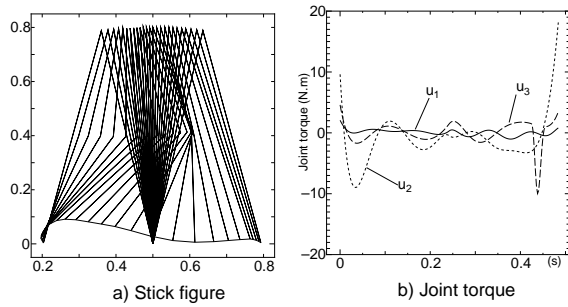


Figure 7: Computation results on $u_3 = 0$ and $t_2 = 0.10s$

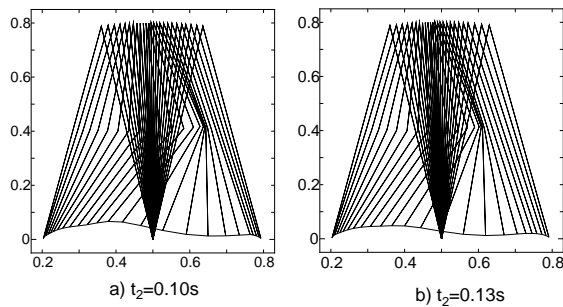


Figure 8: Stick figures (no constraint)

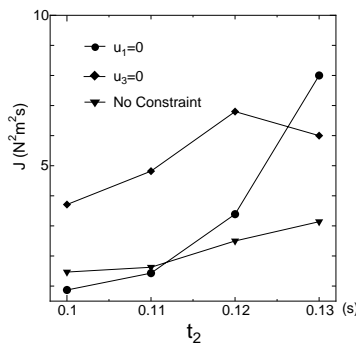


Figure 9: Performance index function value

timal trajectory planning method adopted in this paper is an effective tool to solve the walking motion and joint control torque for a 3-DOF biped walking mechanism.

(2) Under the constraint condition $u_1 = 0$, the period t_2 in the second section has a great influence on the results. When $t_2 = 0.10s$, the energy consumption is the lowest among all examples. In this case, the one step period $t_1 + t_2 = 0.586s$. It is very close to the human walking period, which is about 0.6s. Therefore the corresponding joint motion trajectory is considered to be close to human walking locomotion. This confirms the validity of the inverted pendulum model of human leg system, in which the ankle is a passive joint.

(3) The under-actuated control system is more sensitive to the boundary condition than the full-actuated system. If the suitable boundary condition is adopted, the natural cyclic motion with the

lowest energy consumption can be realized in the under-actuated control system.

References

- [1] T. Mita et al., Realization of a High Speed Biped Using Modern Control Theory, *Int. J. Control*, **40-1**(1984),107-119.
- [2] J. Furusho and M. Masubuchi, Control of a Dynamical Biped Locomotion System for Steady Walking, *J. of Dynamic System, Measurement and Control, Trans. of ASME*, **108**-June(1986),111-118.
- [3] C. Shin, Analysis of the Dynamics of a Biped Robot with Seven Degrees of Freedom, *Proc. of the 1996 IEEE Int. Con. on Robotics and Automation*, Minneapolis, Minnesota-April(1996), 3008-3013.
- [4] A. Sano, Dynamic Biped Walking by Using Skillfully a Gravity Field (Challenge to a Human Walking), *J. of the Robotics Society of Japan*, **11-3**(1993), 354-359.
- [5] H. Miura et al., Dynamic Walk of a Biped, *Int. J. of Robotics Research*, **3-2**(1984), 60-74.
- [6] Jerry Pratt and Gill Pratt, Exploiting Natural Dynamics in the Control of a Planar Bipedal Walking Robot, *Proc. of the 36th IEEE Annual Allerton Conf. on Communication, Control and Computing*, Monticello, Illinois, Sept. 1998.
- [7] Tad McGeer, Passive Dynamic Walking, *Int. J. of Robotics Research*, **9-2**(1990), 62-82.
- [8] K. Ono and T. Okada, Self-Excited Vibratory Actuator (1st Report, Analysis of Two-Degree-of-Freedom Self-Excited System), *Trans. of the JSME*, **60-577**, C(1994a), 92-99.
- [9] K. Ono and T. Okada, Self-Excited Vibratory Actuator (2nd Report, Self-Excitation of Insect Wing Model) *Trans. of the JSME*, **60-579**, C(1994b),117-124.
- [10] K. Ono and T. Okada, Self-Excited Vibratory Actuator (3rd Report, Biped Walking Mechanism by Self-Excitation) *Trans. of the JSME*, **60-579**, C(1994c),125-132.
- [11] K. Ono et al., Self-Excitation of Biped Locomotion Mechanism, *Proc. of the 1999 JSME Con. on Robotics and Mechatronics*(CDROM 2P1-41-093), Tokyo, 1999.
- [12] A. Imadu and K. Ono, Optimal Trajectory Planning Method for a System That Includes Passive Joints (1st Report, Proposal of a Function Approximation Method), *Trans. of the JSME*, **64-618**, C(1998),516-522.